

Hollowing of MnO Nanocrystals Triggered by Metal Cation Replacement: Implications for the Electrocatalytic Oxygen Evolution Reaction

*Original*

Hollowing of MnO Nanocrystals Triggered by Metal Cation Replacement: Implications for the Electrocatalytic Oxygen Evolution Reaction / Wu, C., Dang, Z., Pasquale, L., Wang, M., Colombo, M., De Trizio, L., Manna, L.. - In: ACS APPLIED NANO MATERIALS. - ISSN 2574-0970. - 4:6(2021), pp. 5904-5911. [10.1021/acsnm.1c00819]

*Availability:*

This version is available at: 11583/2991239 since: 2024-10-03T10:02:08Z

*Publisher:*

American Chemical Society

*Published*

DOI:10.1021/acsnm.1c00819

*Terms of use:*

This article is made available under terms and conditions as specified in the corresponding bibliographic description in the repository

*Publisher copyright*

ACS postprint/Author's Accepted Manuscript

This document is the Accepted Manuscript version of a Published Work that appeared in final form in ACS APPLIED NANO MATERIALS, copyright © American Chemical Society after peer review and technical editing by the publisher. To access the final edited and published work see <http://dx.doi.org/10.1021/acsnm.1c00819>.

(Article begins on next page)

## All-Dielectric Compact Superstrates for High-Gain Resonant-Cavity Antennas: Designs & Measurements

Affan A. Baba<sup>1</sup>, Raheel M. Hashmi<sup>1</sup>, Karu P. Esselle<sup>1</sup> and Ladislav Matekovits<sup>2</sup>  
<sup>1</sup>School of Engineering, Macquarie University, Sydney, NSW, 2109, Australia  
<sup>2</sup>Department of Electronics and Telecommunication, Politecnico di Torino, Italy  
**(Special Session)**

### Abstract

This paper presents the designs and measurements of two compact single-layer all-dielectric resonant-cavity antennas (RCAs). Both the antennas are compact (*footprint*  $< 5.5\lambda_0^2$ ) and low in profile (overall *height*  $< 0.9\lambda_0$ ). The first RCA consists of a single-layer partially reflecting superstrate (PRS) in which thickness and permittivity vary from the center towards the edge of the PRS. Four commercially available dielectric materials are used to achieve this permittivity variation. This RCA demonstrates a measured peak directivity of 20.7 dBi and its 3dB directivity bandwidth extends from 12.75-19 GHz, which is 57% at the center frequency. The second RCA, made out of a single dielectric material demonstrates a measured peak directivity of 20.3 dBi and its measured 3dB directivity bandwidth is 55.9%. This class of compact single-layer RCAs, with a directivity bandwidth product per unit area (DBP/A) of greater than 1200, successfully overcomes the trade-off between directivity, bandwidth, profile and footprint and breaks the challenging barrier that has existed for RCAs over the last decade (and other planar high-gain antennas).

**Keywords**—RCAs; High-Gain; Large-Bandwidth; Planar Antennas; Partially Reflecting Superstrate; EBG Resonator Antenna.

### 1. Introduction

With the advent of 5G approaching our doorstep, significant volumes of data are expected to be generated by the future wireless networks. In order to handle such large volumes of data, many wireless transceivers would require the use of wideband antennas combined with software-defined-radio (SDR), which is expected to reduce the size as well as cost of the transceivers. For medium-to-long distance wireless links, directional antennas form a very important requirement. With the mm-wave spectra being extensively explored for future broadband communications, there is a lot of interest in exploring compact, wideband antennas that can be designed and adapted for mm-wave communications, while minimizing fabrication tolerances during the mass fabrication process. Resonant cavity antennas (RCA) are an excellent candidate for such applications. A classical

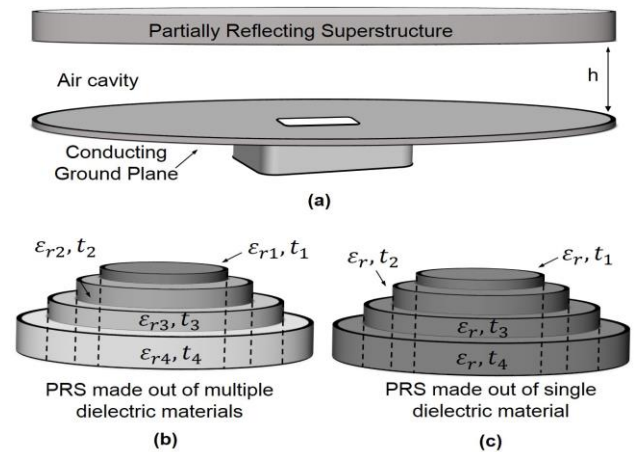


**Figure 1.** General configuration of an RCA with single-layer all-dielectric single-layer PRS. The single-layer PRS can either be made out of (b) multiple dielectric materials or (c) a single dielectric material.

RCA, in its most general form, can be formed by placing a partially reflecting superstrate (PRS) over a conducting ground plane, forming an air-filled cavity in-between [1–11]. RCAs can provide directional radiation with a only a single-feed point, as opposed to microstrip patch antenna arrays, and have a planar, compact configuration, as opposed to horn antennas, which are rather bulky and high profile.

In this paper, we present a recently developed, new class of RCAs with two example antennas and their measured results. Both the RCAs use a single layer PRS, made out of commercially available dielectric materials. We analyze the configuration of each of these RCAs and their fabrication methods. Key considerations are presented while adapting the design to mm-wave bands, which are often overlooked and can cause substantial degradation in the performance of antennas.

### 2. RCA Configurations

Fig. 1 shows the general configuration of an RCA. Two possible PRSs are shown, which may be used in place of the PRS to form the RCA. In the first RCA, we

References	Peak Directivity (dBi)	Bandwidth (%)	Height ( $\lambda_0$ )	Footprint ( $\lambda_0^2$ )	DBP	DBP/A	Superstrate Type	Year
[15]	20.3	55.9	0.88	4.9	5990	1222	Single-dielectric	2018
[14]	20.7	57.0	0.89	5.3	6580	1241	Stepped multi-dielectric	2017

**TABLE I.** Measured performance of RCA prototypes with multi-dielectric and single-dielectric superstrates.

use a PRS that is made out of multiple dielectric materials. The materials used in this case are Rogers 6010 ( $\epsilon_{r1} = 10.2$ ,  $\tan \delta = 0.0023$ ), Rogers TMM10 ( $\epsilon_{r1} = 9.2$ ,  $\tan \delta = 0.0022$ ), Rogers RO3006 ( $\epsilon_{r1} = 6.15$ ,  $\tan \delta = 0.0020$ ) and Rogers RO4003 ( $\epsilon_{r1} = 3.55$ ,  $\tan \delta = 0.0031$ ), from the inner to outermost section. A customize Speed-constrained Multi-objective Particle Swarm Optimization was implemented in MATLAB and linked with CST Microwave Studio to obtain optimum value for the width and thickness of each dielectric sections in the PRS. This optimization led to an RCA with significantly improved radiation characteristics [13-14].

The second stepped PRS shown in Fig. 1 is made out of a single dielectric material Rogers 3010 ( $\epsilon_r = 10.2$ ,  $\tan \delta = 0.0022$ ). The thickness of the PRS ( $t_1$ ,  $t_2$ ,  $t_3$  and  $t_4$ ) reduces in four steps from center towards the edge. The parametric study carried out on the thickness and width of each section in the PRS led to an RCA with a high gain and an extremely large bandwidth [15]. Here it is important to point out that, in order to design the discussed PRS, rigorous full-wave analyses were conducted, since the classic design approaches involving unit-cell optimizations or transmission-line modeling assume a periodic structure extends to infinity in the transverse plane. Such unit-cell methods are not applicable here. On the other hand, a detailed study to differentiate the multi-dielectric and single-dielectric superstrates from lens antennas is presented in [14-16].

### 3. Experimental Results and Discussion

The first RCA prototype made out of a PRS with permittivity variation exhibited a measured peak directivity of 20.7 dBi and a 3dB directivity bandwidth extending from 10.75 – 19 GHz, which is 57% at the center frequency. As shown in Table I, the directivity bandwidth product (DBP) of this RCA is 6580, which is almost three times the best figures for RCAs. The total area of this RCA is  $5.3\lambda_0^2$  and its overall height is  $0.89\lambda_0$  at the lowest operating frequency. On the other hand, as shown in Table I, the RCA prototype made out of a PRS with single dielectric material exhibited a high measured directivity of 20.3 dBi and its 3dB directivity bandwidth

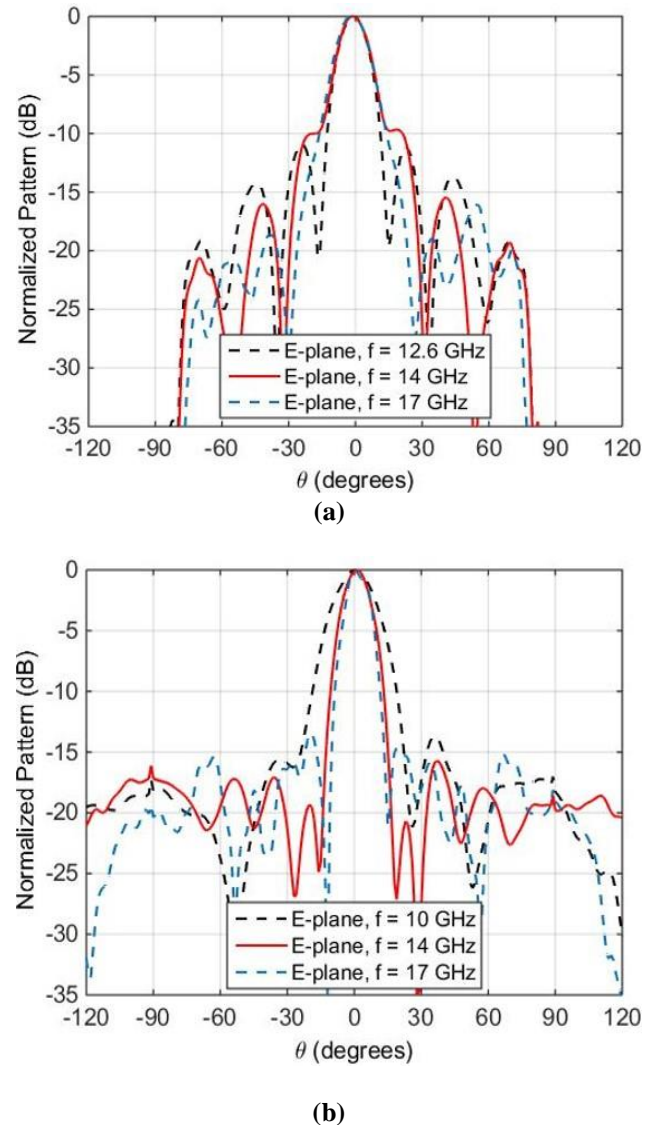


**Figure 2.** Measured radiation pattern of RCAs with (a) the multi-dielectric superstrate and (b) the single-dielectric superstrate.

is 55.9%. The total area and overall height of this RCA are  $4.9\lambda_0^2$  and  $0.88\lambda_0$ , respectively, at the lowest operating frequency. The measured E-plane radiation patterns of both the RCAs at three different frequencies are given in

Figure 2. Here it is important to mention that, over the entire operating band, the measured SLL value in the E-plane for both the RCAs remains below -9dB whereas this value for the other wideband RCAs rises up to -4dB in the E-plane. This class of RCAs has excellent potential for use at mm-wave spectra. Firstly, a single feed point substantially minimizes the complexity and losses associated with feeding networks required in case of arrays. Secondly, the use of only dielectric materials removes any metallization induced tolerances and losses. However, it is worth pointing out that the tolerance in relative permittivity values of commercially available dielectric materials should be considered in the design. Subtractive manufacturing and milling can be commonly used to fabricate the RCAs presented in this paper, and it is easy to overlook the tolerances and variation of permittivity in different commercially dielectric sheets, due to variations in manufacturing process. These variations, although negligible at microwave frequencies (X-band and Ku-band), can become reasonably high at mm-wave frequencies (e.g. V-band). In our experience, such variations lead to pronounced shifts in the operating bandwidths, and thus, in side-lobe levels of the resulting antennas.

#### 4. Conclusion

Designs and measurements of two compact resonant-cavity antennas are studied. It is demonstrated that a high gain greater than 20 dBi along with an extremely large 3dB directivity bandwidth (>55%) can be achieved using compact size RCAs. To the best of our knowledge, no RCA prototype has demonstrated such a large gain bandwidth, or a DBP of 6580. The total height and footprint of both the antennas are less than  $0.9\lambda_0$  and  $5.5\lambda_0^2$ , respectively. These compact antennas are highly suitable for mm-wave medium-to high-gain space-limited applications where large directivity/gain bandwidth is required.

#### 7. References

1. G. V. Trentini, "Partially reflecting sheet arrays," *IRE Trans. Antennas Propag.*, vol. 4, no. 4, pp. 666–671, Oct. 1956.
2. A. R. Weily, K. P. Esselle, T. S. Bird, and B. C. Sanders, "Dual resonator 1-D EBG antenna with slot array feed for improved radiation bandwidth," *Microwaves, Antennas & Propagation, IET*, vol. 1, pp. 198-203, 2007.
3. K. Singh, M. P. Abegaonkar and S. K. Koul, "Ultrathin miniaturized meta-surface for wide band gain enhancement," *2017 IEEE Asia Pacific Microwave Conference (APMC)*, Kuala Lumpur, 2017, pp. 383-386.
4. F. Wu and K. M. Luk, "Wideband high-gain open resonator antenna using a spherically modified, second-order cavity," *IEEE Trans. Antennas Propag.*, vol. 65, no. 4, pp. 2112–2116, April 2017.
5. A. Lalbakhsh, M. U. Afzal and K. P. Esselle, "Multiobjective Particle Swarm Optimization to Design a Time-Delay Equalizer Metasurface for an Electromagnetic Band-Gap Resonator Antenna," in *IEEE Antennas and Wireless Propagation Letters*, vol. 16, pp. 912-915, 2017.
6. N. Wang, J. Li, G. Wei, L. Talbi, Q. Zeng, and J. Xu, "Wideband Fabry Perot resonator antenna with two layers of dielectric superstrates," *IEEE Antennas and Wireless Propag. Lett.*, vol. 14, pp. 229–232, 2015.
7. Y. Yu, W. Wu, Z. Zong and D. Fang, "A Wire Metamaterial Loaded Resonant Cavity Antenna Using 3-D Printing Technology," in *IEEE Antennas and Wireless Propagation Letters*. doi: 10.1109/LAWP.2018.2851204.
8. A. R. Weily, L. Horvath, K. P. Esselle, B. Sanders, and T. Bird, "A planar resonator antenna based on a woodpile EBG material," *IEEE Trans. Antennas Propag.*, vol. 53, pp. 216-223, 2005.
9. N. Nguyen-Trong, H. H. Tran, T. K. Nguyen and A. M. Abbosh, "Wideband Fabry–Perot Antennas Employing Multilayer of Closely Spaced Thin Dielectric Slabs," in *IEEE Antennas and Wireless Propagation Letters*, vol. 17, no. 7, pp. 1354-1358, July 2018.
10. R. M. Hashmi and K. P. Esselle, "A class of extremely wideband resonant cavity antennas with large directivity-bandwidth products," *IEEE Trans. Antennas Propag.*, vol. 64, no. 2, pp. 830–835, 2016.
11. M. A. Al-Tarifi, D. E. Anagnostou, A. K. Amert, and K. W. Whites, "The puck antenna: A compact design with wideband, high-gain operation," *IEEE Trans. Antennas Propag.*, vol. 63, no. 4, pp. 1868–1873, Apr. 2015.
12. R. Orr, G. Goussetis, and V. Fusco, "Design method for circularly polarized Fabry–Perot cavity antennas," *IEEE Trans. Antennas Propag.*, vol. 62, no. 1, pp. 19–26, Jan. 2014.
13. A. A. Baba, R. M. Hashmi, K. P. Esselle and A. R. Weily, "Two-level optimization of a stepped dielectric superstrate to increase gain of a resonant cavity antenna," *2017 International Conference on Electromagnetics in Advanced Applications (ICEAA)*, Verona, 2017, pp. 1131-1133.
14. A. A. Baba, R. M. Hashmi, and K. P. Esselle, "Achieving a large gain-bandwidth product from a compact antenna," *IEEE Transactions on Antennas and Propagation*, vol. 65, no. 7, pp. 3437-3446, 2017.
15. A. A. Baba, R. M. Hashmi, K. P. Esselle and Andrew R. Weily, "Compact High-Gain Antenna With Simple

All-Dielectric Partially Reflecting Surface," IEEE Transactions on Antennas and Propagation, vol. 66, no. 8, pp. 4343-4348, 2018.

16. R. M. Hashmi, A. A. Baba and K. P. Esselle, "Transverse Permittivity Gradient (TPG) Superstrates or Lens: A Critical Perspective," 2018 IEEE International Symposium on Antennas and Propagation and USNS-URSI Radio Science Meeting, Boston, Massachusetts (accepted).